ELSEVIER

Chemical Engineering Journal 144 (2008) 227–234

Chemical Engineering Journal

www.elsevier.com/locate/cej

Effect of channel opening angle on the performance of structured packings

S.J. Luo [a], W.Y. Fei [a,*], X.Y. Song [a], H.Z. Li [b]

[a] *The State Key Laboratory of Chemical Engineering, Department of Chemical Engineering, Tsinghua University, Beijing 100084, China*

[b] *Laboratoire des Science du Génie Chimique, CNRS-ENSIC-INPL, 54001 Nancy, France*

Received 11 October 2007; received in revised form 10 January 2008; accepted 15 January 2008

Abstract

Structured packings are efficient gas–liquid contacting devices and have been widely used in many industrial applications for decades. Unfortunately the channel opening angle, an important geometrical parameter of structured packing, has received only little attention until now. In this work, the effect of channel opening angle on the performance of the column containing structured packing was investigated both numerically and experimentally. The simulation results show that the pressure drop can decrease substantially and the liquid maldistribution can be effectively reduced when the channel opening angle decreases from 90° to 20°. The simulation is in quite good agreement with the experiments. In addition, a new modified structured packing was validated according to total reflux distillation experiment. It was shown that the pressure drop of the new packing could reduce by 35% and mass transfer efficiency could increase by 13% compared to the Mellapak packing having the same specific surface area.

Keywords: Structured packing; Channel opening angle; Mass transfer; Pressure drop

1. Introduction

Structured packings have many advantages over random packings and tray columns, and are widely used in mass transfer processes, such as distillation and absorption. For example, columns containing structured packings can provide larger surface area for gas–liquid contact and better hydrodynamic behavior, including lower pressure drop and higher load capacity, etc. Billet [1] showed that structured packings could reduce maldistribution, which is often observed in column with conventional packings. A growing demand for more efficient structured packings appears in various industrial applications, such as the challenging problem of carbon dioxide capture and storage. Therefore, it is necessary to optimize the geometrical parameters that influence the hydrodynamic behavior and mass transfer performance with the aim to improve their capacity and efficiency.

The packing with inclination angle of 60° was designed, and the experimental evidence [2–4] illustrated that this packing can lead to a significant capacity increase, while the capacity gain is roughly equal to the percentage decrease of the mass transfer efficiency. Optiflow [5], which was developed by Sulzer Chemtech, permits a considerable performance enhancement. However, the increase in the mass transfer efficiency was only observed for rather low liquid loads. In addition, Optiflow has a limited flexibility and relatively high manufacturing cost [6]. Although inserting flat plate between corrugated sheets can produce a lower pressure drop, the mass transfer performance was rather poor due to the severe liquid maldistribution [7]. Further work is still required in order to investigate possible structured packings with higher performance.

Recently, an excessive liquid accumulation at the interface between packing elements observed by Suess and Spiegel [8] was identified as a limiting factor for capacity enhancement [9]. Therefore a modified geometry at the top and/or bottom ends of each standard element was considered as a simple but effective alternative. Fig. 1 illustrates some typical modifications. FLEXIPC-HC differs from the original Flexipac only in the bottom part of each element that is flattened for approximate height of 20 mm. And then the new packing displays a higher hydraulic diameter and enables a smoother flow direction change for the gas phase. Sulzer's MELLAPAK-PLUS packing is

* Corresponding author. Tel.: +86 10 62789637; fax: +86 10 62789637.
E-mail address: fwy-dce@tsinghua.edu.cn (W.Y. Fei).

1385-8947/$ – see front matter © 2008 Elsevier B.V. All rights reserved.
doi:10.1016/j.cej.2008.01.026

Nomenclature

a	top side length of trapezoid channel (m)
a_p	specific surface area of packing (m^{-1})
b	half of the corrugation base length (m)
B	width of liquid film (m)
F_g	gas load factor ($m\,s^{-1}\,(kg\,m^{-3})^{0.5}$)
g	gravity, constant parameter = 9.8 $m\,s^{-2}$
$\vec{g}$	gravity field ($m\,s^{-2}$)
g_x	component of gravity along the x-axis for vertical plate ($m\,s^{-2}$)
g_y	component of gravity along the y-axis for vertical plate ($m\,s^{-2}$)
g_z	component of gravity along the z-axis for vertical plate ($m\,s^{-2}$)
g''_x	component of gravity along the x-axis for corrugated sheet ($m\,s^{-2}$)
g''_y	component of gravity along the y-axis for corrugated sheet ($m\,s^{-2}$)
g''_z	component of gravity along the z-axis for corrugated sheet ($m\,s^{-2}$)
h	corrugation height (m)
H	height of the packing element (m)
N	number of theoretical stage per unit height (m^{-1})
N_T	theoretical stage
p	pressure
ΔP	bed pressure drop (Pa)
ΔP_C	pressure drop caused by crossing junction (Pa)
ΔP_{dry}	dry-bed pressure drop (Pa)
s	corrugation side length (m)
t	time (s)
T_b	boiling point (°C)
U	effective gas velocity ($m\,s^{-1}$)
$\vec{v}$	velocity field ($m\,s^{-1}$)
Y	dimensionless distance from liquid entrance
Z	packed height (m)

Greek letters

α	the corrugation inclination angle (°)
β	the channel opening angle (°)
ε	packing void fraction
η	liquid film thickness (m)
μ	viscosity (Pa s)
ρ	density ($kg\,m^{-3}$)
σ	surface tension ($N\,m^{-1}$)

Subscripts

q	the qth phase

different from its conventional geometry in which the top and bottom ends of each corrugated sheet are bent to be vertical. This kind of geometry creates a relatively short transition zone and produces lower pressure drop. Other packings have a smooth bend of one-third bottom to increase continuously the hydraulic diameter, such as Montz B1-M. The packing with reduced crimp height at the bottom part [10] or with height-staggered sheets [11] are also a beneficial geometry modification. However, the experimental results [6,12,13] indicated that these modified packings achieve capacity increase, on the other hand lead to a certain deterioration of mass transfer efficiency.

By reviewing the modifications to the structured packings, it is found that the triangular flow channel and the basic geometrical parameters did not change much. This might be explained by the fact that the optimum geometry of corrugated sheets seemed to be reached for a long time [14]. While the contact area, which is the common interface shared by neighboring fluid channels, determines the gas–gas interfaces, and has influence over the pressure drop of packed column. The channel opening angle has a close relationship with the contact area, so it has strong effect on the hydrodynamic and mass transfer performance of column equipped with structured packings. However, the packing manufacturers and researchers still pay little attention to this key parameter, and there is no report about the effect of channel opening angle on the hydrodynamic and mass transfer efficiency of structured packings.

In this work, the relationship between the channel opening angle and the performance of corrugated packing is addressed both numerically and experimentally. At the same time, a new type of corrugated packing is also investigated.

2. Model

2.1. Spatial geometry of the corrugated sheet

Structured packings are made of many corrugated sheets, which are installed at a certain angle α from the horizontal and form triangular flow channels (Fig. 2). The special geometry of corrugated sheet ensures that the inclined plate of triangular flow channel is developed after two rotations. Fig. 3 shows one of rotation ways. First, the vertical gray plate and the coordinate (x, y, z) rotate $(90 - \alpha)$ degree around negative x-axis. After rotation, the coordinate (x, y, z) changes to (x', y', z'). Second, the gray plate rotates $(-\beta/2)$ degree around positive y'-axis in the coordinate (x', y', z'). Here α means the channel inclination angle, and β is the channel opening angle. After two rotations, the spatial position of the gray plane in Fig. 3(c) is exactly the same as the white plane in Fig. 2.

2.2. Weight component analysis

The gravity component over the surface of the corrugated sheet quantitatively was analyzed as follows. It was supposed that the coordinate of an arbitrary point P in the vertical plate is (x^1, x^2, x^3) (Fig. 3(a)), and then the coordinate changes to (y^1, y^2, y^3) and (z^1, z^2, z^3), respectively, after two rotations (Fig. 3(b) and (c)). The relationship between (x^1, x^2, x^3), (y^1, y^2, y^3) and (z^1, z^2, z^3) can be expressed using Eqs. (1) and (2).

$$\begin{pmatrix} y^1 \\ y^2 \\ y^3 \end{pmatrix} = A \begin{pmatrix} x^1 \\ x^2 \\ x^3 \end{pmatrix} \tag{1}$$

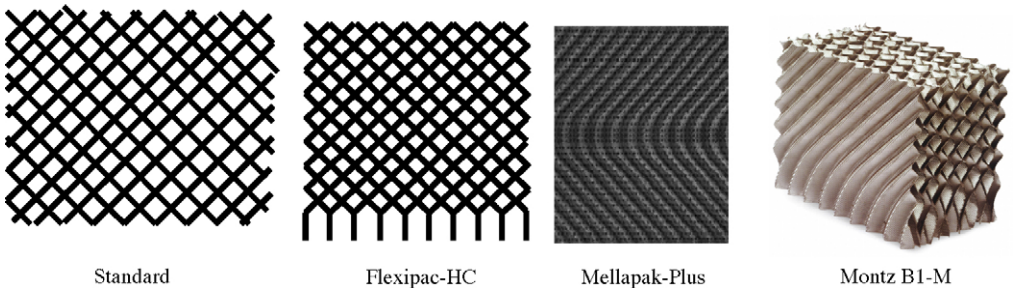

Fig. 1. Different modifications of structured packings.

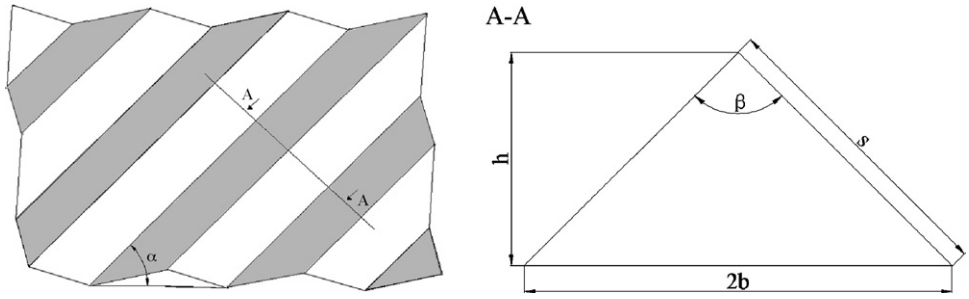

Fig. 2. Corrugated sheet of structured packing.

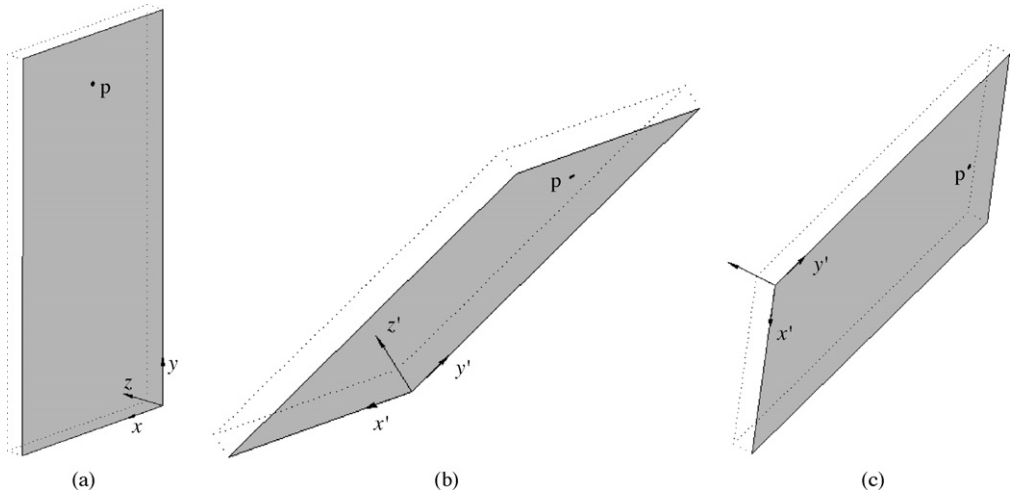

Fig. 3. Rotation steps.

$$\begin{pmatrix} z^1 \\ z^2 \\ z^3 \end{pmatrix} = B \begin{pmatrix} y^1 \\ y^2 \\ y^3 \end{pmatrix} \tag{2}$$

where

$$A = \begin{pmatrix} 1 & 0 & 0 \\ 0 & \sin\alpha & -\cos\alpha \\ 0 & \cos\alpha & \sin\alpha \end{pmatrix},$$

$$B = \begin{pmatrix} \cos(\beta/2) & 0 & -\sin(\beta/2) \\ 0 & 1 & 0 \\ \sin(\beta/2) & 0 & \cos(\beta/2) \end{pmatrix}$$

so

$$\begin{pmatrix} z^1 \\ z^2 \\ z^3 \end{pmatrix} = BA \begin{pmatrix} x^1 \\ x^2 \\ x^3 \end{pmatrix} \tag{3}$$

where

$$BA = \begin{pmatrix} \cos(\beta/2) & -\sin(\beta/2)\cos\alpha & -\sin(\beta/2)\sin\alpha \\ 0 & \sin\alpha & -\cos\alpha \\ \sin(\beta/2) & \cos(\beta/2)\cos\alpha & \cos(\beta/2)\sin\alpha \end{pmatrix}$$

According to tensor analysis, the gravity component in different coordinate can be expressed by Eq. (4).

$$g^{i''} = \frac{\partial z^i}{\partial x^j} g^j, \quad i = 1, 2, 3, \qquad j = 1, 2, 3 \tag{4}$$

The weight component on the vertical plate (Fig. 3(a)) can be described by relation (5), and then the different gravity on the inclined plate of corrugated sheet can be calculated using Eq. (6) according to Eqs. (3)–(5).

$$\begin{pmatrix} g_x \\ g_y \\ g_z \end{pmatrix} = \begin{pmatrix} 0 \\ -g \\ 0 \end{pmatrix} \tag{5}$$

$$\begin{pmatrix} g_x'' \\ g_y'' \\ g_z'' \end{pmatrix} = -g \begin{pmatrix} -\sin(\beta/2)\cos\alpha \\ \sin\alpha \\ \cos(\beta/2)\cos\alpha \end{pmatrix} \tag{6}$$

These components are illustrated in Fig. 4, where n is the surface normal, g_x'', g_y'' and g_z'' are the different gravity components over the inclined plate, g_0 is the vector sum of g_x'' and g_y''.

2.3. Computed geometry

The computed geometry in the present work is similar to the plate in Fig. 3(a). The body forces at three different directions are given by Eq. (6) so that the simulation results can throw insight into the liquid flow over the surface of structured packing. However, the simulation results were shown on the plate similar to the one in Fig. 3(c). The inclination angle α is fixed as 45°; and the channel opening angle β is specified as 90° and 20°, respectively.

The computed domain was generated using the GAMBIT tool with the dimension of 20 mm × 40 mm × 4 mm (Fig. 5). Liquid was supplied to the upper part of the model system through a 0.5 mm narrow slit perpendicular to the wetted plate. Different velocity values were set corresponding to different flow rates at the liquid inlet. In this paper, the gas phase was considered as stagnant with zero velocity, and without affecting the liquid flow. The existing experimental results [15] showed that this assumption is valid for low vapor load. At the outlet, gauge

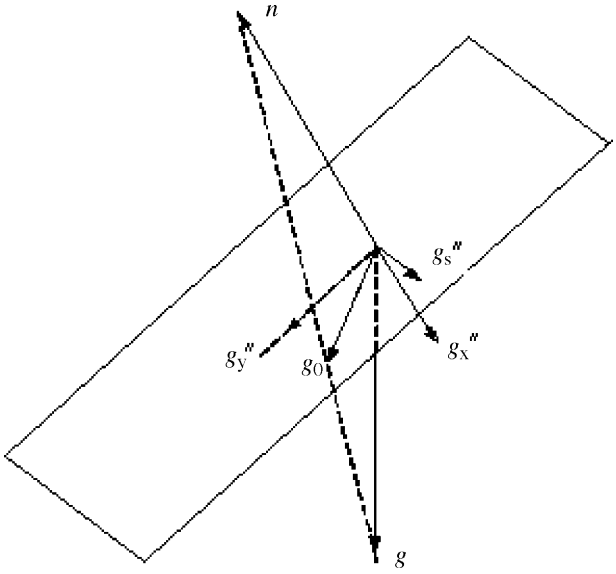

Fig. 4. Weight component over the corrugated sheet.

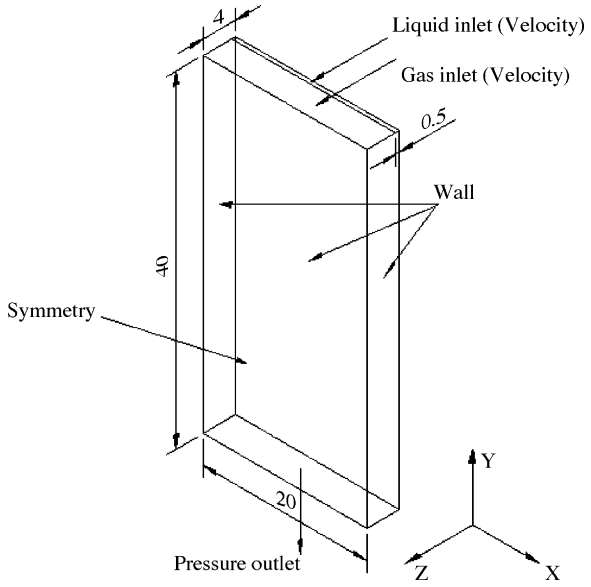

Fig. 5. Geometry of computed dimension.

pressure value was settled as zero, and the backflow volume fraction of liquid phase equal to zero. The back plane, which means the surface of corrugated sheet here, and two side planes were defined as walls. As for the front plane, symmetry boundary condition was implemented.

2.4. CFD model

The simulation of the liquid flow over the surface of corrugated sheet was performed with the multiphase flow volume of fluid (VOF) model within FLUENT [16]. This model was developed by Hirt and Nichols [17] for two or more immiscible phases where the position of the interface between the fluids is of interest. It is a surface tracking technique applied to a fixed Eulerian. The application of the VOF model includes stratified flows, free-surface flows, etc. It has been successfully used to predict the liquid flow on an inclined solid surface [18,19].

In the VOF model, a single momentum equation was solved throughout the domain, and the resulting velocity field was shared among the phases. The momentum equation, shown below, is dependent on the volume fractions of all phases through the properties ρ and μ.

$$\frac{\partial}{\partial t}(\rho\vec{v}) + \nabla\cdot(\rho\vec{v}\vec{v}) = -\nabla p + \nabla\cdot[\mu(\nabla\vec{v} + \nabla\vec{v}^T)] + \rho\vec{g} \tag{7}$$

The properties appearing in the transport equations were determined by the presence of the component phases in each control volume. Here the phases were represented by the subscripts 1 and 2. If the volume fraction of the second phase was to be tracked, and the density and viscosity in each cell were then given by

$$\rho = \alpha_2\rho_2 + (1-\alpha_2)\rho_1 \tag{8}$$

$$\mu = \alpha_2\mu_2 + (1-\alpha_2)\mu_1 \tag{9}$$

The interface tracking was accomplished by the solution of a continuity equation for the volume fraction of the different phases. For the qth phase, this equation has the following form:

$$\frac{\partial \alpha_q}{\partial t} + \vec{v} \cdot \nabla \alpha_q = 0, \quad q = 1, 2 \tag{10}$$

The primary-phase volume fraction was not solved by volume fraction equation, but computed under the following constraint:

$$\sum_{q=1}^{n} \alpha_q = 1, \qquad n = 2 \tag{11}$$

Water and air were considered as liquid phase and gas phase, respectively, in this study. Numerical simulation was carried out in an unsteady state with time step varying from 10^{-6} s at the beginning of the calculations up to 10^{-3} s. The geometric reconstruction scheme was used for the VOF estimation. PRESTO scheme was adopted to interpolate the pressure value at the faces. Pressure–velocity coupling was realized using PISO scheme. As for the discretization of momentum equation, the first-order upwind scheme was applied. Initially, the domain was filled with gas, and zero values were set for all other variables. In the present work, all the simulations were run by means of FLUENT code version 6.2. A double precision segregated solver was chosen to solve the above set of equations.

3. Experiment

The distillation experimental setup used in this study is shown in Fig. 6. The column had the internal diameter of 0.1 m and the packing's height of 0.8 m. All runs were carried out with alcohol/water system at the ambient pressure under the total reflux conditions.

The structured packings considered in this work are made of wire gauze, and the major dimensions are gathered in Table 1. The geometry of smaller channel opening angle (SCOA) packing [20], a new patented corrugated packing, was different from the traditional structured packing. The main characteristic of the new packing was that the triangular flow channels (Fig. 2) are changed to trapezoid ones (Fig. 7). Here the angle between the two non-parallel sides extension was defined as the channel opening angle β.

The hydrodynamic performance in terms of pressure drop per unit height ($\Delta p/\Delta z$) and mass transfer efficiency, which represents the number of theoretical stage per unit height (N), were plotted against the vapor load (F-factor), respectively. The F-factor was defined as the product of superficial vapor velocity and the square root of the vapor density.

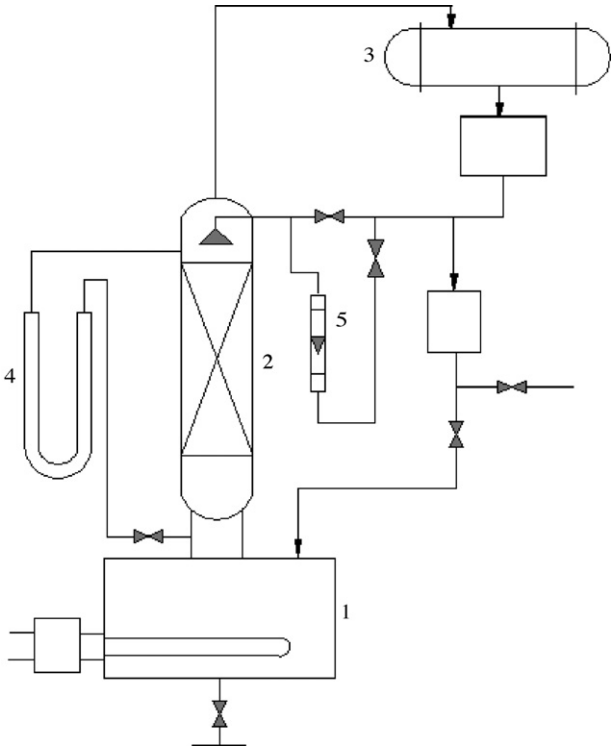

Fig. 6. Experimental setup. (1) Bottom of the column; (2) column containing structured packings; (3) condenser; (4) U-type pressure manometer and (5) flowmeter.

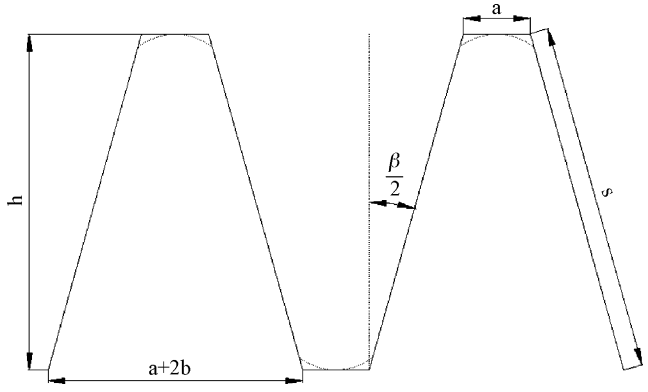

Fig. 7. Trapezoid fluid channel of smaller channel opening angle (SCOA) packing.

The number of theoretical stage per unit height can be calculated using the following equation:

$$N = \frac{N_T}{Z} \tag{12}$$

where Z is the total packing's height, N_T is the number of theoretical stage, which can be deduced from the ladder graphic

Table 1
Characteristic dimensions of structured packings considered in this work

Packing type	a_p (m^2/m^3)	α (°)	β (°)	a (m)	b (m)	h (m)	s (m)	H (m)	ε
Mellapak	900	45	90	0	0.0032	0.0032	0.0045	0.05	0.97
SCOA	900	45	20	0.001	0.0014	0.008	0.0081	0.05	0.97

Table 2
Physical properties of the alcohol and water system

	Alcohol	Water
Molecular formula	C_2H_6O	H_2O
Molecular weight	46	18
Density, ρ (kg/m^3) (20 °C)	789	998
Boiling point, T_b (°C) (101.3 kPa)	78.3	100
Surface tension, $\sigma \times 10^3$ (N m^{-1}) (20 °C)	22.8	72.2

method. The vapor–liquid equilibrium curve was fitted by means of the NRTL model, where the parameters [21] are given in the following. The procedure was implemented in FORTRAN.

$$\ln \gamma_1 = x_2^2 \left[\frac{\tau_{21} G_{21}^2}{(x_1 + x_2 G_{21})^2} + \frac{\tau_{12} G_{12}}{(x_2 + x_1 G_{12})^2} \right] \quad (13)$$

$$\ln \gamma_2 = x_1^2 \left[\frac{\tau_{12} G_{12}^2}{(x_2 + x_1 G_{12})^2} + \frac{\tau_{21} G_{21}}{(x_1 + x_2 G_{21})^2} \right] \quad (14)$$

where $\tau_{12} = (g_{12} - g_{22})/RT$, $\tau_{21} = (g_{21} - g_{11})/RT$, $G_{12} = \exp(\alpha_{12}\tau_{12})/RT$, $G_{21} = \exp(\alpha_{12}\tau_{21})/RT$, $(g_{12} - g_{22}) = -2.5594$, $(g_{21} - g_{11}) = -56.2391$, $\alpha_{12}(\alpha_{21}) = 0.3007$.

The physical properties of the alcohol and water are gathered in Table 2.

4. Results and discussion

4.1. Hydrodynamic analysis

By dividing the dry-bed pressure drop into three parts: the gas–gas collision and friction in the crisscross junction; the direction change in the interlayer junction, and the form drag near the wall zones, computational fluid dynamics (CFD) was used to compute the different components of the overall pressure drop. Further details of the dry-bed pressure drop model and the computational procedures are available elsewhere [22].

According to the literatures [22,23], pressure drop due to the gas–gas collision and friction in crisscross junction makes substantial contribution to the total pressure drop, meanwhile these pressure losses do not contribute significantly to mass transfer [7]. Therefore, reducing this pressure drop component could lead to capacity increase without affecting adversely the mass transfer efficiency, or vice versa.

Fig. 8 shows the simulated pressure drops resulting from different crisscross junctions. Obviously, there is a substantial reduction for SCOA packing than Mellapak packing. As expected, the dry-bed pressure drop of SCOA packing is distinctly lower than Mellapak packing (Fig. 9). The main reason can be conjectured from contact area, which is 1.44×10^{-5} m^2 and 4.1×10^{-5} m^2 for SCOA packing and Mellapak packing, respectively. A smaller contact area can reduce the gas–gas collision probability, and then results in pressure drop decrease.

According to total reflux distillation experiment, measured pressure drop curves shown in Fig. 10 illustrate the same hydrodynamic performance. SCOA packing can result in 35% pressure drop decrease compared with Mellapak packing.

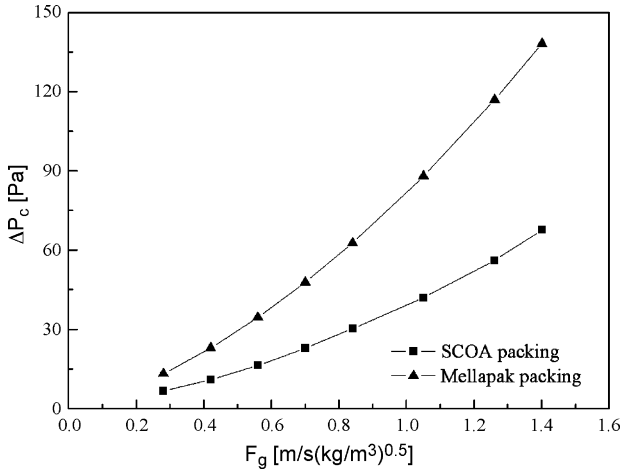

Fig. 8. Comparison of the pressure drop coming from crisscross junction.

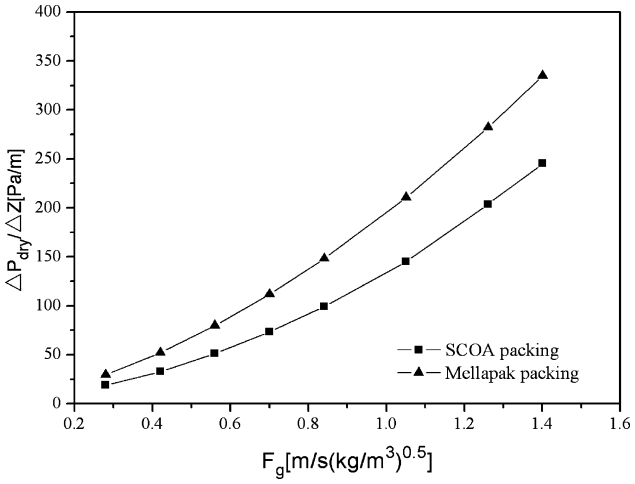

Fig. 9. Simulated dry-bed pressure drop per unit height.

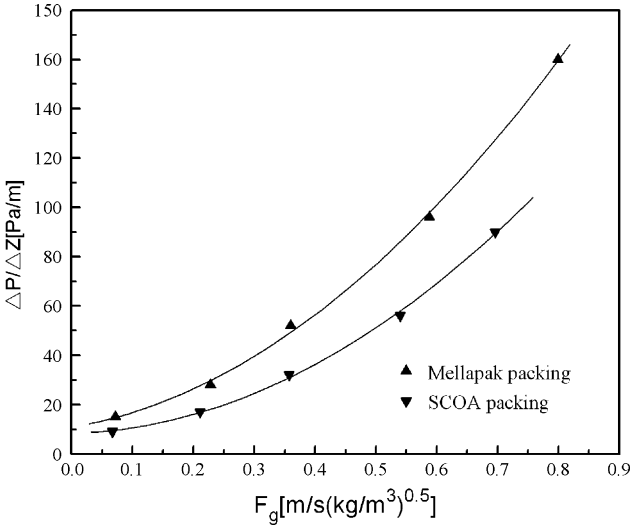

Fig. 10. Experimental pressure drop per unit height.

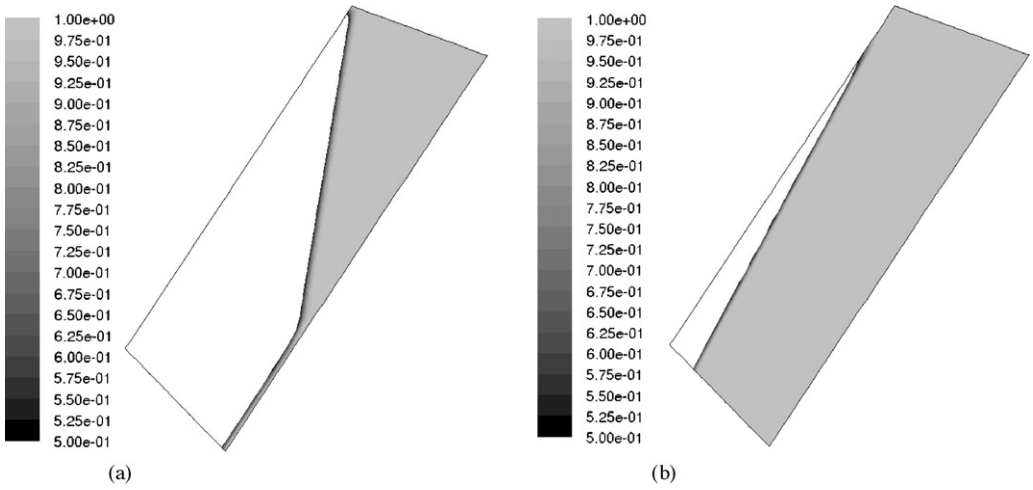

Fig. 11. VOF contours for water at different corrugated sheets. (a) Channel opening angle is 90° and (b) channel opening angle is 20°.

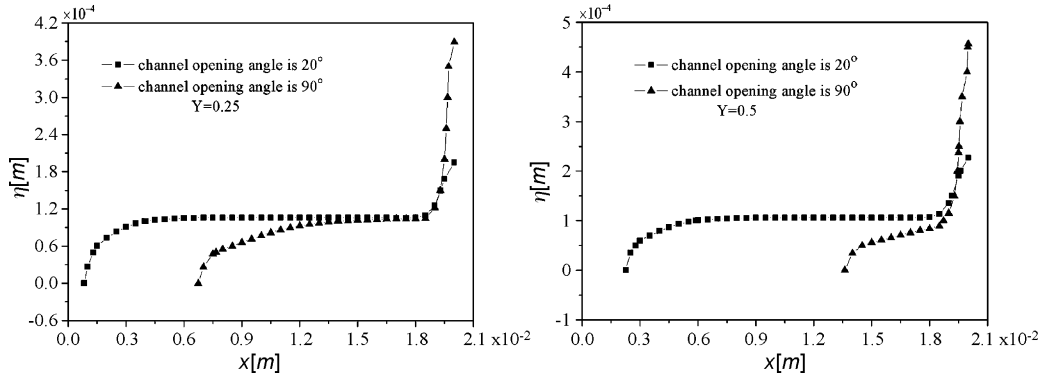

Fig. 12. Film thickness profile at different places.

4.2. Mass transfer efficiency analysis

Liquid distribution onto the surface of structured packing is crucial to the performance of packed towers used in heat and mass transfer applications [24]. Although there are several models developed to predict mass transfer and hydrodynamic performance of structured packings [25,26], the wetting characteristics and spatial liquid distribution inside the packings were recognized as a major missing knowledge [27]. Further experimental and theoretical investigations are required. In the following, the simulated results of liquid film flow over the surface of structured packing are addressed to throw insight into the understanding of the liquid spreading and distribution mechanism, as well as the mass transfer efficiency estimation.

Fig. 11 shows the VOF contours for water at different corrugated sheets. The isosurface where VOF equals 0.5 represents the gas–liquid interface. Clearly the maldistribution problem is severe for the packing with channel opening angle 90°. On the contrary, liquid phase can almost completely wet the surface of corrugated sheet when the channel opening angle decreases to 20°. Here, it is worth pointing out that the simulated result in Fig. 11(a) corresponds well to the experimental data [28].

The film thickness profiles obtained from the simulation at water volume fraction of 0.5 are shown in Fig. 12. Here Y is the dimensionless distance from liquid inlet to the interested position. Fluid accumulates evidently in one side wall and thins near another one. In addition, the film width differs distinctly for different packing sheets. Because of wide spreading and

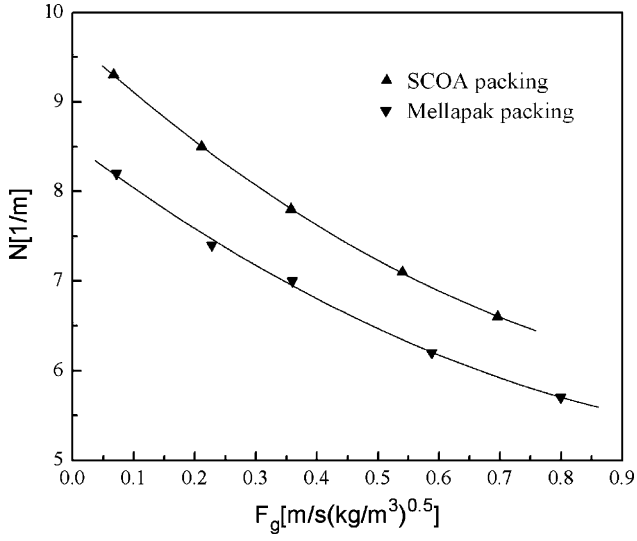

Fig. 13. Comparison of the mass transfer efficiency between SCOA and Mellapak packings.

neglected accumulation of the liquid phase, the packing with channel opening angle 20° lead to a larger interfacial area. It is obviously helpful to improve mass transfer efficiency.

Fig. 13 shows the number of theoretical stage per unit height getting from distillation experiment. As expected, the mass transfer performance get much better after decreasing the channel opening angle. The mass transfer efficiency gain for SCOA packing is around 13%, and the relative gain is quite satisfactory and stable with vapor load increase.

5. Conclusions

The effect of channel opening angle on the hydrodynamic and mass transfer performance of structured packing was investigated both numerically and experimentally. Based on the simulation results, decreasing channel opening angle can largely reduce "useless" pressure drop stemming from the interaction of crossing gas streams, and lead to a better hydrodynamic performance. Meanwhile it is also a hopeful way to improve the mass transfer efficiency. The CFD simulation is in good agreement with experiments.

According to the total reflux distillation experiment, the SCOA packing, after low cost modifications with respect to standard packing, features in more than 35% pressure drop decrease and 13% mass transfer efficiency gain compared to conventional structured packings with same specific surface area. These results are very promising for various applications, such as vacuum distillations and absorption.

References

[1] R. Billet, Packed Column Analysis and Design, Ruhr-Universitat Bochum, Department of Thermal Separation Processes, Bochum, Germany, 1989.
[2] Z. Olujic, A.F. Seibert, J.R. Fair, Influence of corrugation geometry on the performance of structured packings: an experimental study, Chem. Eng. Process. 39 (2000) 335–342.
[3] H.J. Verschoof, Z. Olujic, J.R. Fair, A general correlation for prediction the loading point of corrugated sheet structured packings, Ind. Eng. Chem. Res. 38 (1999) 3663–3669.
[4] J.R. Fair, A.F. Seibert, M. Behrens, et al., Structured packing performance—experimental evaluation of two predictive models, Ind. Eng. Chem. Res. 39 (2000) 1788–1796.
[5] L. Spiegel, M. Knoche, Influence of hydraulic conditions on separation efficiency of Optiflow, Chem. Eng. Res. Des. 77 (1999) 609–612.
[6] Z. Olujic, H. Jansen, B. Kaibel, et al., Stretching the capacity of structured packings, Ind. Eng. Chem. Res. 40 (2001) 6172–6180.
[7] M. Behrens, P.P. Saraber, H. Jansen, et al., Performance characteristics of a monolith-like structured packing, Chem. Biochem. Eng. Q. 15 (2001) 49–57.
[8] P. Suess, L. Spiegel, Hold-up of Mellapak structured packings, Chem. Eng. Process. 31 (1992) 119–124.
[9] Z. Olujic, B. Kaibel, H. Jansen, et al., Distillation column internals/configurations for process intensification, Chem. Biochem. Eng. Q. 17 (2003) 301–309.
[10] P. Bender, A. Moll, Modifications to structured packings to increase their capacity, Chem. Eng. Res. Des. 81 (2003) 58–67.
[11] J.F. Billingham, M.J. Loakett, Development of a new generation of structured packings for distillation, Chem. Eng. Res. Des. 77 (1999) 583–587.
[12] G. Parkinson, G. Ondrey, Packing towers, Chem. Eng. 106 (1999) 39–43.
[13] Z. Olujic, A.F. Seibert, B. Kaibel, et al., Performance characteristics of a new high capacity structured packing, Chem. Eng. Process. 42 (2003) 55–60.
[14] L. Spiegel, W. Meier, Distillation columns with structured packings in the next decade, Chem. Eng. Res. Des. 81 (2003) 39–47.
[15] R. Billet, Packed Tower in Processing and Environmental Technology, VCH, Weinheim, 1995.
[16] 6.2 Fluent, User's Guide, Fluent Inc., 2000.
[17] C.W. Hirt, B.D. Nichols, Volume of fluid (VOF) method for the dynamics of free boundaries, J. Comput. Phys. 39 (1981) 201–225.
[18] H. Andreas, A. Ilja, R. Jens-Uwe, W. Guenter, Fluid dynamics in multiphase distillation processes in packed towers, Comp. Chem. Eng. 29 (2005) 1433–1437.
[19] G. Fang, C.J. Liu, X.G. Yuan, G.C. Yu, CFD simulation of liquid film flow on inclined plates, Chem. Eng. Technol. 27 (2004) 1095–1104.
[20] W.Y. Fei, X.Y. Song, CN Patent, CN2787298Y.2005-10-26.
[21] J. Gmeshling, V. Onken, N.J.R. Rarey, Vapor–liquid Equilibrium Data Collection, DECHEMA, Frankfurt, 1988.
[22] S.J. Luo, X.Y. Song, W.Y. Fei, Relationship between channel opening angle and dry-bed pressure drop of structure packing, J. Chem. Ind. Eng. (China) 58 (2007) 2764–2769.
[23] Z. Olujic, Development of a complete simulation model for predicting the hydraulic and separation performance of distillation columns equipped with structured packings, Chem. Biochem. Eng. Q. 11 (1997) 31–46.
[24] A. Ataki, P. Kolb, U. Buehlmann, H.J. Bart, Wetting performance and pressure drop of structured packings: CFD and experiment, Inst. Chem. Eng. Symp. Ser. 152 (2006) 534–543.
[25] G.F. Woerlee, J. Berends, Z. Olujic, J.D. Graauw, A comprehensive model for the pressure drop in vertical pipes and packed columns, Chem. Eng. J. 84 (2001) 367–379.
[26] A. Shilkin, E.Y. Kenig, A new approach to fluid separation modeling in the columns equipped with structured packings, Chem. Eng. J. 110 (2005) 87–100.
[27] A. Ataki, H.J. Bart, Experimental and CFD simulation study for the wetting of a structured packing element with liquids, Chem. Eng. Technol. 29 (2006) 336–347.
[28] B. Szulczewska, Z. Ireneusz, G. Andrzej, Liquid flow on structured packing: CFD simulation and experimental study, Chem. Eng. Technol. 26 (2003) 580–584.